Axial Ligation in Blue-Copper Proteins. A W-Band Electron Spin Echo Detected Electron Paramagnetic Resonance Study of the Azurin Mutant M121H

M. van Gastel,[†] G. W. Canters,[‡] H. Krupka,[§] A. Messerschmidt,[§] E. C. de Waal,[‡] G. C. M. Warmerdam,[‡] and E. J. J. Groenen*,[†]

Contribution from the Centre for the Study of Excited States of Molecules, Huygens Laboratory, Leiden University, P.O. Box 9504, 2300 RA, Leiden, The Netherlands, Gorlaeus Laboratories, Leiden University, P.O. Box 9502, 2300 RA Leiden, The Netherlands, and Max-Planck-Institut für Biochemie, Am Klopferspitz 18A, D-82152 Martinsried bei München, Germany

Received September 15, 1999. Revised Manuscript Received December 2, 1999

Abstract: The green Met121His mutant of the blue-copper protein azurin has been investigated by pulsed electron paramagnetic resonance (EPR) spectroscopy at 95 GHz on a single crystal. The axial histidine is more strongly bound to copper than the methionine for the wild-type protein. The **g** tensor of M121H is found to be virtually axial and the *z* principal axis perpendicular to the plane spanned by copper and the nitrogens of the ligating histidines 46 and 117. The direction of the *x* axis is close to the bond direction from copper to the nitrogen of histidine 46. Theoretical analysis of the axiality and the orientation of the principal axes shows that the wave function of the unpaired electron on copper, largely d_{xy} for blue-copper proteins, acquires some d_{yz} character for M121H. Comparison of these results with data for wild-type azurin and the mutant M121Q provides insight into the subtle relation between the electronic and the geometric structure of blue-copper sites.

Introduction

The metal site in blue-copper proteins has intrigued scientists ever since the observation of the remarkably strong visible absorption around 600 nm and the small copper hyperfine splitting in the $g_{||}$ region of the electron paramagnetic resonance (EPR) spectrum. Nevertheless, a full understanding of the relation between the electronic and the geometric structure is still lacking. The X-ray structures[1−4] of blue-copper proteins reveal a highly conserved copper site. The copper is ligated by three strong equatorial ligands, i.e., two nitrogens of two histidines and the sulfur of a cysteine. A closer look at the X-ray structures reveals differences in geometry among the family of blue-copper proteins that are responsible for subtle variations in the electronic properties observed in the EPR and electronic absorption spectra. For *Pseudomonas aeruginosa* azurin, the structure of the copper site is almost trigonal with a distance of copper to the equatorial plane of only 0.08 Å. The strong visible absorption of this protein is centered around 625 nm[5] and the **g** tensor is nearly axial.[6] The electronic absorption and EPR spectra of plastocyanin[7] are similar to those of azurin although the distance of copper to the NNS plane amounts to 0.34 Å[2]. This distance is close to that for pseudoazurin (0.43 Å), a protein that is blue but shows significant rhombicity in the EPR spectrum.

Besides the equatorial ligands, a weak axial ligand, usually the sulfur of a methionine, is present at a distance to the copper of about 2.6−3.2 Å. Recently, several mutants of azurin have been prepared where the axial methionine has been mutated,[8−10] among them M121Q and M121H of *Alcaligenes denitrificans* azurin with a glutamine and a histidine at position 121. The distance of the fourth ligand (oxygen, nitrogen) to copper is reduced to about 2.3 Å in both cases, and the distances of copper to the NNS plane are 0.26 and 0.56 Å, respectively. The structure and spectra of M121Q[11] are found to mimic those of stellacyanin,[3] a native blue-copper protein with the oxygen of a glutamine as its axial ligand. Interestingly, the EPR spectrum of M121Q is rhombic and that of M121H even more axial than that of azurin. On the other hand, the electronic absorption spectra of both mutants show absorption around 450 nm, which for M121H becomes so strong relative to the absorption around 625 nm that this mutant has a green color.

The electronic structure of the blue-copper proteins has been

[†] Huygens Laboratory, Leiden University.
[‡] Gorlaeus Laboratories, Leiden University.
[§] Max-Planck-Institut für Biochemie.

(1) Nar, H.; Messerschmidt, A.; Huber, R.; van de Kamp, M.; Canters, G. W. *J. Mol. Biol.* **1991**, *221*, 765−772.
(2) Colman, P. J.; Freeman, H.; Guss, J. M.; Murata, M.; Norris, V. A.; Ramshaw, J. A. M.; Venkatappa, M. P. *Nature* **1978**, *272*, 319−324.
(3) Hart, P. J.; Nersissian, A. M.; Herrmann, A. G.; Nalbandyan, R. M.; Valentine, J. S.; Eisenberg, D. *Protein Sci.* **1996**, *5*, 2175−2183.
(4) Adman, E. T.; Turley, S.; Bramson, R.; Petratos, K.; Banner, D.; Tsernoglou, D.; Beppu, T.; Wanatabe, H. *J. Biol. Chem.* **1989**, *264*, 87−99.
(5) Horio, T. *J. Biochem.* **1958**, *45*, 195−205.
(6) Coremans, J. W. A.; Poluektov, O. G.; Groenen, E. J. J.; Canters, G. W.; Nar, H.; Messerschmidt, A. *J. Am. Chem. Soc.* **1994**, *116*, 3097−3101.
(7) Penfield, K. W.; Gewirth, A. A.; Solomon, E. I. *J. Am. Chem. Soc.* **1985**, *107*, 4519−4529.
(8) Bonander, N.; Karlsson, B. G.; Vanngard, T. *Biochemistry* **1996**, *35*, 2429−2436.
(9) Romero, A.; Hoitink, C. W. G.; Nar, H.; Huber, R.; Messerschmidt, A.; Canters, G. W. *J. Mol. Biol.* **1993**, *229*, 1007−1020.
(10) Kroes, S. J.; Hoitink, C. W. G.; Andrew, C. R.; Ai, J.; Sanders-Loehr, J.; Messerschmidt, A.; Hagen, W. R.; Canters, G. W. *Eur. J. Biochem.* **1996**, *240*, 342−351.
(11) Messerschmidt, A.; Prade, L.; Kroes, S. J.; Sanders-Loehr, J.; Huber, R.; Canters, G. W. *Proc. Natl. Acad. Sci. U.S.A.* **1998**, *95*, 3443−3448.

10.1021/ja993357f CCC: $19.00
Published on Web 02/23/2000

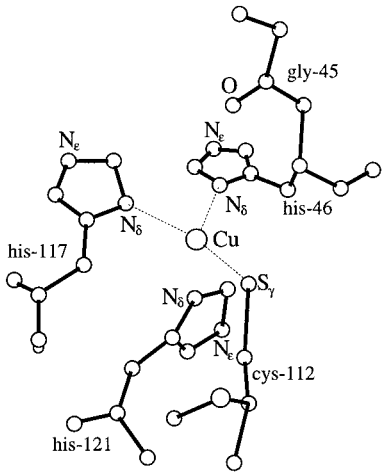

Figure 1. Copper site of the M121H mutant of azurin.

studied by various quantum chemical techniques.[7,12−14] The wave function of the unpaired electron is best described by a d orbital on the copper (d_{xy} in our axes system, vide supra), which is π-antibonding to a 3p orbital of the sulfur of the cysteine and σ-antibonding to the lone pair orbitals of the nitrogens of the histidines. This wave function leads to an axial EPR spectrum, and the proteins derive their blue color from an electronic absorption that has been ascribed to a sulfur to copper π charge-transfer transition.[7] For stellacyanin, the rhombicity in the EPR spectrum has been attributed to a small admixture of d_{z^2} orbital into the wave function of the unpaired electron.[15,16] The trigonal blue-copper site is calculated to be intrinsically stable,[17] approximately as stable as tetragonal copper sites. However, to judge the quality of the calculated wave functions, more quantitative experimental data are necessary.

EPR spectroscopy allows the investigation of the electronic structure of the oxidized proteins, and in particular, the advent of high-frequency techniques has largely enhanced the potential of EPR for such systems. From pulsed 95 GHz electron spin echo (ESE) studies on single crystals of azurin,[6] the complete **g** tensor has been obtained, as well as insight into the delocalization of the wave function of the unpaired electron over the copper-bound histidines.[18,19] A first attempt to investigate the axial ligation concerned M121Q.[20]

Here, we report on an ESE-detected EPR study of the azurin mutant M121H. The geometry of the copper site of M121H is shown in Figure 1. From the EPR study of M121H, the complete **g** tensor has been determined. The *z* principal axis of the **g** tensor is found to be perpendicular to the plane going through copper and the nitrogens of the strongly bound histidines. Analysis of the **g** tensor based on a simple model provides new insight into the relation between rhombicity and the binding of the axial ligand. For M121H, d_{yz} character mixes into the wave function of the unpaired electron. Comparison of the EPR spectra of M121H with those of azurin and M121Q allows a discussion of the link between the electronic and geometric structures of blue-copper sites.

Materials and Methods

The expression and purification procedure for the M121H mutant of azurin is described elsewhere.[10] Crystallization of M121H has been performed according to the procedure outlined in ref 11. The typical dimensions of the M121H crystal are $0.2 \times 0.2 \times 0.2$ mm^3, and the pH of the buffer of the crystals was 6.5.

The EPR experiments have been performed at a temperature of 1.2 K on a home-built ESE spectrometer at 95 GHz. The spectrometer has been described in ref 21 except for the fact that the microwave bridge has been replaced by one from the Department of Microwave Equipments for Millimeter Waveband ESR Spectroscopy in Donetsk, Ukraine. An M121H crystal was mounted in a capillary tube with an inner and outer diameter of 0.60 and 0.84 mm, respectively, and the edges of the tube were closed with sealing wax. The electron spin echo was generated by a two-pulse sequence with typical lengths of 60 and 90 ns, respectively, and the pulse separation was 300 ns. The repetition rate of the pulse sequence was 14 Hz. The intensity of the echo was recorded by a boxcar integrator and fed to a computer via an ADC. The EPR spectrum for each orientation of the magnetic field with respect to the M121H crystal has been recorded by monitoring the height of the echo and scanning the strength of the magnetic field. Because the spectrometer allows for a rotation of the direction of the magnetic field in a plane containing the capillary and a rotation of the capillary about its own axis, all orientations of the magnetic field with respect to the crystal can be selected without remounting the crystal.

Results

The ESE-detected EPR spectrum at 95 GHz of a frozen solution of the M121H mutant of azurin is shown in Figure 2a. The field of maximum absorption in the EPR spectrum corresponds to $g_{yy} = 2.053 \pm 0.002$. The rhombicity is too small to be resolved. Two features are present in the $g_{||}$ region of the EPR spectrum with *g* values of 2.257 ± 0.002 and 2.29 ± 0.01. The copper hyperfine structure is not visible because of *g*-strain broadening.

For single crystals of M121H, ESE-detected EPR spectra have been recorded for various orientations of the magnetic field $\vec{B}_0$ with respect to the crystal. Examples are shown in the upper traces of parts b−f of Figure 2, which illustrate that the spectrum depends strongly on the direction of $\vec{B}_0$. The orientations of the principal axes *x* and *z* that correspond to the g_{xx} and g_{zz} values of the **g** tensors of the different molecules in the unit cell and the orientations of the crystallographic axes have been found according to the procedure described in refs 6 and 20. Figure 2b shows the EPR spectrum for the M121H crystal with $\vec{B}_0$ aligned to an *x* axis. The spectrum is characterized by relatively narrow bands in the high-field part of the spectrum and broader ones in the low-field part. The resonance at the highest field observed in this spectrum is outside the magnetic field range of the spectrum of the frozen solution. The directions of 16 principal *x* axes corresponding to a g_{xx} value of 2.031 have been determined with an experimental accuracy of ±3°. The directions of 12 *z* axes have been identified, albeit with a limited accuracy of ±7° due to the fact that the low-field resonances are broad and weak. Eight of the stationary fields of resonance

(12) Gewirth, A. A.; Solomon, E. I. *J. Am. Chem. Soc.* **1988**, *110*, 3811−3819.
(13) Larsson, S.; Broo, A.; Sjölin, L. *J. Phys. Chem.* **1995**, *99*, 4860−4865.
(14) Pierloot, K.; de Kerpel, J. O. A.; Ryde, U.; Roos, B. O. *J. Am. Chem. Soc.* **1997**, *119*, 218−226.
(15) Gewirth, A. A.; Cohen, S. L.; Schugar, H. J.; Solomon, E. I. *Inorg. Chem.* **1987**, *26*, 1133−1146.
(16) de Kerpel, J. O. A.; Pierloot, K.; Ryde, U.; Roos, B. O. *J. Phys. Chem. B* **1998**, *102*, 4638−4647.
(17) Olsson, M. H. M.; Ryde, U.; Roos, B. O.; Pierloot, K. *JBIC, J. Biol. Inorg. Chem.* **1998**, *3*, 109−125.
(18) Coremans, J. W. A.; Poluektov, O. G.; Groenen, E. J. J.; Canters, G. W.; Nar, H.; Messerschmidt, A. *J. Am. Chem. Soc.* **1997**, *119*, 4726−4731.
(19) Coremans, J. W. A.; Poluektov, O. G.; Groenen, E. J. J.; Canters, G. W.; Nar, H.; Messerschmidt, A. *J. Am. Chem. Soc.* **1996**, *118*, 12141−12153.
(20) Coremans, J. W. A.; Poluektov, O. G.; Groenen, E. J. J.; Warmerdam, G. C. M.; Canters, G. W.; Nar, H.; Messerschmidt, A. *J. Phys. Chem.* **1996**, *100*, 19706−19713.
(21) Disselhorst, J. A. J. M.; van der Meer, H.; Poluektov, O. G.; Schmidt, J. *J. Magn. Reson. A* **1995**, *115*, 183−188.

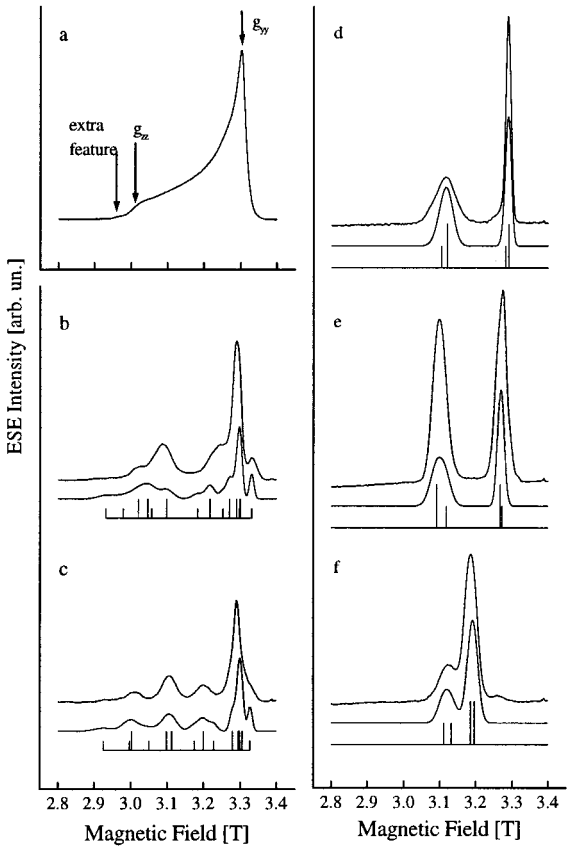

Figure 2. W-band ESE-detected EPR spectra of a frozen solution of M121H (a) and a single crystal of M121H (b−f) at 1.2 K. For spectra in (b) and (c), the magnetic field is approximately parallel to an *x* and a *z* axis, respectively. For spectra in (d), (e), and (f) the magnetic field is approximately parallel to the *a*, *b*, and c crystallographic axes, respectively.

correspond to $g_{zz} = 2.256$ and four to $g_{zz} = 2.321$. The latter four directions differ about 8° from four of the former directions. In Figure 2c, an EPR spectrum is represented for which $\vec{B}_0$ is almost aligned to both a *z* axis with $g = 2.256$ and a *z* axis with $g = 2.321$. The direction of $\vec{B}_0$ differs only 6° from that for the spectrum in Figure 2b, which explains the resemblance of both spectra.

The EPR spectra for $\vec{B}_0$ parallel to the *a*, *b*, or *c* crystallographic axes are shown in parts d−f of Figure 2. The identity of the crystallographic axes has been determined by comparing the spectra for M121H with those for the M121Q mutant for which an additional X-ray experiment was performed following the EPR study.[20] The spectra consist of two bands, but a closer look reveals additional features. The spectrum for $\vec{B}_0 \| a$ (Figure 2d) shows a shoulder on the low-field band, the high-field band in the spectrum for $\vec{B}_0 \| b$ (Figure 2e) is asymmetric, and the spectrum for $\vec{B}_0 \| c$ shows an additional weak band at about 3.26 T (Figure 2f).

Besides the spectra for which $\vec{B}_0$ is parallel to the *a*, *b*, or *c* axis or to *x* or *z* axes, spectra have been acquired for many other orientations of $\vec{B}_0$ with respect to the crystal. These data have been included in the simulations of the EPR spectra.

Data Analysis

A. ESE-Detected EPR Spectra. The M121H crystal belongs to space group $C222_1$ with two molecules in the asymmetric unit and eight asymmetric units in the unit cell.[9,11] The C-centering operation relates two groups of four asymmetric units by translational symmetry. Because this operation does not affect the orientation of a molecule, the number of magnetically inequivalent molecules is eight, and therefore, eight resonances are expected in the ESE-detected EPR spectrum for an arbitrary orientation of the magnetic field. If the magnetic field is aligned to a crystallographic axis, the asymmetric units are magnetically equivalent and two resonances are expected. However, the EPR spectra for the M121H crystal in parts b−f of Figure 2 do not conform to this picture. Because 16 directions of principal *x* axes and 12 directions of principal *z* axes have been found, spectral simulations within the constraints set by the space group and the number of magnetically inequivalent molecules in the unit cell cannot adequately describe the experimental spectra.

To interpret the EPR spectra, we assume that two conformations of the copper site in the M121H crystal contribute to the spectra. This assumption is suggested by three observations. First, signals were found in the single-crystal spectra that are outside the range spanned by the *g* values that characterize the EPR spectrum of the frozen solution. Second, two distinct g_{zz} values have been found in the EPR spectra of the crystal. Third, the refined X-ray data for M121H indicate different average geometries of the copper site of the two molecules in the asymmetric unit. The most striking difference concerns the distance between copper and the sulfur of cysteine-112 of 2.25 Å for one and 2.06 Å for the other molecule in the asymmetric unit.[11] This difference is on the edge of the experimental accuracy, but if real, such variations may well give rise to different **g** tensors.

Under the assumption that two electronically different conformations of the copper site with tensors **g** and **g′** contribute, the EPR spectra have been analyzed as follows. The 16 magnetically inequivalent molecules in the unit cell (8 for each conformation) lead to 16 resonances in the EPR spectra. The electronic Zeeman interaction determines the fields of resonance of 8 molecules according to

$$B_{\mathrm{res}} = \frac{h\nu}{\mu_\beta \sqrt{\sum_i (g_{ii} \cos \phi_i)^2}} \qquad (1)$$

where $i = x, y, z$, h is Planck's constant, ν is the microwave frequency, μ_β is the Bohr magneton, and ϕ is the angle between the axis *i* of the **g** tensor of the particular molecule and $\vec{B}_0$. For the other eight molecules, a similar formula was used where g_{ii} was replaced by g'_{ii} in order to take into account the differences in *g* values between the two conformations. Copper hyperfine interaction was not explicitly considered because it is not resolved in the EPR spectra at 95 GHz. On the basis of the relative intensities of the resonances at low field in the EPR spectra with $\vec{B}_0 \| z$ corresponding to g_{zz} or g'_{zz}, the conformations with **g** and **g′** tensors are assumed to be present in a 2 to 1 ratio. First, the g_{ii} values and the corresponding directions of the principal axes for the dominant conformation of the copper site are fit to the most intense bands in 60 experimental EPR spectra recorded at various orientations of $\vec{B}_0$. The fit was performed under the constraints implied by the space group, giving rise to two groups of four *x* and *z* directions for which the axes within one group are symmetry-related by 180° rotations about the crystallographic axes. Subsequently, the g'_{ii} values and the corresponding directions of the principal axes are fit under the same constraints to the remaining, less intense bands in the experimental spectra. The results are summarized in Table 1. The calculated fields of resonance for those directions of $\vec{B}_0$ that correspond to the experimental spectra in Figure 2

Table 1. *g* Values and Principal Axes (*xyz*) Directions of the Four Nonsymmetry-Related **g** Tensors with Respect to the Crystallographic Axes (*abc*) in the M121H Crystal[a]

$g_{xx} = 2.0507 \pm 0.0006$, $g_{yy} = 2.0555 \pm 0.0006$, $g_{zz} = 2.2645 \pm 0.0006$

	g tensor **1**				**g** tensor **2**		
	a	*b*	*c*		*a*	*b*	*c*
x	0.7739	0.2297	−0.5902	*x*	−0.2207	0.7139	−0.6646
y	−0.6046	0.5455	−0.5805	*y*	−0.6324	−0.6235	−0.4598
z	0.1886	0.8060	0.5610	*z*	−0.7426	0.3188	0.5891

$g'_{xx} = 2.034 \pm 0.002$, $g'_{yy} = 2.056 \pm 0.002$, $g'_{zz} = 2.321 \pm 0.002$

	g′ tensor **1′**				**g′** tensor **2′**		
	a	*b*	*c*		*a*	*b*	*c*
x	0.5724	0.4796	−0.6651	*x*	−0.4191	0.5817	−0.6972
y	−0.7820	0.5633	−0.2667	*y*	−0.5845	−0.7604	−0.2831
z	0.2467	0.6728	0.6975	*z*	−0.6948	0.2888	0.6586

[a] The *z* directions have an uncertainty of 1°, and the *x* and *y* axes have an uncertainty of 4°. The **g** tensors **1** and **2** occur about twice as often in the crystal as the **g′** tensors **1′** and **2′**.

are represented in the same figure as stick spectra where the long sticks refer to the resonances of the dominant conformation and the short sticks to those of the minor conformation. The middle curves in the panels of Figure 2, which facilitate the comparison of experimental and simulated spectra, are calculated by dressing each stick with a Gaussian line shape of width ΔB given by

$$\Delta B = \sqrt{\sum_i (W_{ii} \cos \phi_i)^2} \qquad (2)$$

where $i = x, y, z$ and W_{ii} are adjustable parameters. The line width tensor, determined by *g* strain and unresolved hyperfine interaction, is assumed to have principal axes parallel to the principal axes of the corresponding **g** tensor. Furthermore, the line width parameters W_{ii} are assumed to be the same for both conformations. The line width parameters used for the simulated spectra in parts b−f of Figure 2 are 12, 12, and 44 mT for W_{xx}, W_{yy}, and W_{zz}. Relaxation and modulation effects, which derive from the use of the ESE method and influence the intensities of the bands in the EPR spectra, are not taken into account in the simulations.[22] Within this limitation, the experimental and simulated spectra are in agreement. The optimized value of g_{zz} differs by 0.009 from the value read from the EPR spectrum, while for g'_{zz} the two values agree. The optimized values of g_{yy} and g'_{yy} differ 0.004 from the *g* value that corresponds to the maximum absorption in the EPR spectrum of the frozen solution, and the optimized g_{xx} and g'_{xx} values differ 0.02 and 0.002 from the ones read from the corresponding spectra. For the **g′** tensor the refined directions of the *x* and *z* axes are within 4° of the directions read from the spectra; for the **g** tensor the differences are 20° and 9°, respectively. These relatively large changes upon refinement will be explained in the discussion section.

B. Orientation of the Principal Axes of the g Tensor with Respect to the Copper Site. The EPR experiment has allowed the determination of the orientation of the principal axes of the **g** tensors of the molecules in the unit cell with respect to the crystallographic axes. Here, the EPR data are combined with results from X-ray diffraction studies in order to find the directions of the principal axes of the **g** tensor with respect to the copper site. We define the ligand geometry of the copper site as the average of the structures reported in the X-ray study for the copper sites of molecules A and B in the asymmetric unit.[11]

The average geometry of the copper site is calculated as follows. First, molecule B is translated such that the coordinates of the copper atom of this molecule coincide with those of molecule A. Second, molecule B is rotated such that the sum over all atoms of the square of the distances between the corresponding atoms of molecules A and B is minimum, and finally, the two structures are added with weights 0.5 to yield the average structure of the protein at position A in the unit cell. The average geometry of the protein molecule at position B is calculated in a similar fashion by superimposing molecule A onto molecule B.

Table 2. Angles (deg) between the Bond Direction of Copper and Its Ligating Atoms in the Average Copper Site of M121H and the Principal Axes of the **g** Tensor (*xyz*)[a]

	1			2			3			4		
	x	*y*	*z*	*x*	*y*	*z*	*x*	*y*	*z*	*x*	*y*	*z*
Cu−N(His-46)	15	105	95	32	58	86	86	129	39	100	80	14
Cu−S(Cys-112)	125	55	126	158	73	104	99	100	166	118	127	130
Cu−N(His-117)	112	158	88	71	133	131	137	54	69	94	19	108
Cu−N(His-121)	76	53	41	91	93	4	8	83	87	35	121	75

[a] The numbers 1, 2, 3, 4 represent the four possible assignments. The average accuracy in the angles is 5°.

The refined directions of the principal axes of the eight **g** tensors have been combined in all possible ways with the orientations of the molecules in the X-ray structure while looking for an assignment such that the angles between the principal axes and the bond directions from copper to its ligating atoms for all eight magnetically inequivalent molecules are equal within the combined accuracy of the EPR and the X-ray experiment. The same has been done for the eight **g′** tensors.

Four assignments of the directions of the principal axes of both the **g** and **g′** tensors with respect to the average copper site are found possible. For the dominant conformation of the copper site these orientations are represented in Table 2, where the angles between the copper−ligand directions and the principal axes of the **g** tensor are given. For the minor conformation, the angles differ about 15° from those presented in Table 2. The average uncertainty in the angles is about 5°.

Discussion

A. g Tensor. The EPR spectra of the M121H crystal reveal two species with notably different *g* values (cf. Table 1). The g_{zz} value of the dominant species is smaller than the g'_{zz} value of the minor species, and the rhombicity of the **g′** tensor is larger. The *g* values ($g_{yy} = 2.0555$ and $g_{zz} = 2.2645$) are similar to those found in the axial EPR spectrum of the frozen solution (2.053 and 2.257) of M121H (cf. Figure 2a). In contrast, the g'_{xx} value is lower than the one observed in the spectrum of the frozen solution. The refined principal directions corresponding to g'_{xx} and g'_{zz} are found to be closest to the experimental directions, differing by only 4°. This is because g'_{xx} is the smallest and g'_{zz} the largest optimized *g* value and experimentally the principal directions have been determined by looking for isolated high-field or low-field resonances in the EPR spectrum. The refined directions of the principal axes that correspond to g_{xx} and g_{zz} differ by 20° and 9° from the experimental ones. The experimental directions have been determined in the same way as those corresponding to g'_{xx} and g'_{zz}, but the EPR spectra reveal effective high-field and low-field resonances due to overlap with the resonances of the species with the **g′** values. This becomes apparent for example in the stick spectrum of Figure 2c for which B_0 is almost parallel to the *z* direction of both a **g** and a **g′** tensor. The extreme low-field resonance in this spectrum, corresponding to g'_{zz}, is isolated, and the low-field resonance of the long sticks, corresponding to g_{zz}, is not.

(22) Mims, W. B.; Peisach, J. *Biochemistry* **1976**, *15*, 3863−3869.

In a previous EPR study of a single crystal of the M121Q mutant of azurin[20] a similar observation was made as here for M121H. Twice as many signals were observed than expected on the basis of the number of magnetically inequivalent molecules in the unit cell. At that time the most plausible explanation for the doubling seemed to be symmetry-lowering upon cooling of the crystal. Following that study, additional low-temperature diffraction experiments have been performed on an M121Q and an M121H crystal and no lowering of symmetry was observed. The analysis of the EPR spectra for M121H presented here indicates that, most probably, also for the M121Q crystal two distinct conformations of the copper site are present. This conclusion does not affect the analysis of the **g** tensor for M121Q as presented in ref 20.

The X-ray study on the M121H crystal[11] revealed that the geometries of the copper sites of the two molecules in the asymmetric unit are different. Consequently, the two distinct **g** tensors may correspond to the two geometries derived from the X-ray data. To determine the directions of the principal axes of the **g** tensor with respect to the copper site, the average geometry of the copper sites of the two molecules in the asymmetric unit had to be taken and the orientation of the **g** and **g′** principal axes was calculated with respect to this geometry. This simplification, necessary in view of the average nature of the X-ray results, eliminates the possibility of investigating the differences between the **g** tensors in terms of minor differences in the geometry of the copper site.

B. g Tensor and the Wave Function of the Unpaired Electron on Copper. The combination of EPR and X-ray data leaves room for four possibile orientations of the principal axes system *xyz* of the **g** tensor with respect to the average copper site. For the dominant species, the angles between the principal axes and the bond directions of copper and its ligating atoms are summarized in Table 2. Here, we will argue that assignment 1 is correct. We base this conclusion on a theoretical analysis of the **g** tensor in relation to the influence of the axial ligand on the orbital of the unpaired electron on copper. In our analysis of the **g** tensor we use a simplified model for the calculation of the spin−orbit coupling corrected wave function. Only the 3d orbitals on copper are taken into account because the spin−orbit coupling at copper is larger than at the lighter atoms. We take the (normalized) wave function for the unpaired electron on copper as

$$|\psi_0\rangle = A\, d_{xy} + B\, d_{yz} + C\, d_{xz} + D\, d_{x^2-y^2} + E\, d_{z^2} \qquad (3)$$

with real coefficients. From perturbation theory, the spin−orbit coupling corrected wave function is calculated according to

$$|\psi_{SOC}\rangle = |\psi_0\rangle + \sum_i |\psi_i\rangle \frac{\langle\psi_i|\lambda\vec{L}\cdot\vec{S}|\psi_0\rangle}{\epsilon_i - \epsilon_0} \qquad (4)$$

where the sum runs over the excited states $|\psi_i\rangle$, λ is the spin−orbit parameter for copper (829 cm^{-1}), and ϵ_0 and ϵ_i are the energies of the ground state and the excited states. Under the approximation that all excited states have the same energy $\Delta\epsilon$ with respect to the ground state,[20] the square of the **g** matrix,[23] up to first order in the perturbation parameter $k \equiv \lambda/\Delta\epsilon$, becomes

$$\mathbf{g}^2 = \begin{bmatrix} g_e^2 + 4g_e k(1 + 3B^2 + 2E^2 + 2\sqrt{3}DE) & 4g_e k(-3BC + 2\sqrt{3}AE) & -4g_e k(3AB + 3CD + \sqrt{3}CE) \\ 4g_e k(-3BC + 2\sqrt{3}AE) & g_e^2 + 4g_e k(1 + 3C^2 + 2E^2 + 2\sqrt{3}DE) & 4g_e k(-3AC + 3BD - \sqrt{3}BE) \\ -4g_e k(3AB + 3CD + \sqrt{3}CE) & 4g_e k(-3AC + 3BD - \sqrt{3}BE) & g_e^2 + 4g_e k(4 - 3C^2 - 3B^2 - 4E^2) \end{bmatrix} \qquad (5)$$

In view of the large g_{zz} value and the presence of a band around 590 nm in the absorption spectrum,[10] we assume that the electronic structure of M121H is similar to that of blue-copper proteins. Theoretical considerations for the blue-copper protein plastocyanin have shown that the wave function of the unpaired electron for such proteins largely concerns a 3d orbital on copper, which is σ-antibonding with the two lone-pair orbitals of the histidyl nitrogens and π-antibonding with a 3p orbital of the sulfur of the cysteine.[24] We define our axes system such that this orbital concerns d_{xy} with the *x* axis bisecting the bond directions from copper to histidines 46 and 117. In case the wave function of the unpaired electron on copper is properly described by the d_{xy} orbital (i.e., $A = 1$, $B = C = D = E = 0$), the model naturally leads to an axial contribution of the spin−orbit coupling on copper to the **g** tensor with the principal *z* axis (which is the eigenvector of the $\mathbf{g}^2$ matrix related to the largest principal value) perpendicular to the *xy* plane.

The binding of an axial ligand introduces a small d_{z^2}, d_{yz}, or d_{xz} character into the wave function of the unpaired electron on copper. For a small d_{z^2} contribution (i.e., $A \gg E$, $B = C = D = 0$), the **g** tensor acquires significant rhombicity via the *xy* and *yx* elements. Within the model

$$|g_{xx} - g_{yy}| = 8\sqrt{3}kAE$$

and is equal to 0.06 for typical values of *k* and *E* of 0.03 and 0.15, which is not compatible with the near-axiality of the **g** tensor of M121H. If, on the other hand, axial binding involves the d_{yz} orbital (i.e., $A \gg B$, $C = D = E = 0$), diagonalization of the $\mathbf{g}^2$ matrix reveals an axial **g** tensor. An admixture of d_{yz} character simply is equivalent to a tilt of the d orbital, and the principal *z* axis remains in the *xz* plane, albeit rotated with respect to the *z* direction by $\arctan B/A$ (admixture of d_{xz} character leads to a similar situation). For a small value of *B* of about 0.15, this tilt is less than 10° and the *z* axis still makes an angle of about 45° with the lobes of the d_{yz} orbital. In other words, the prediction in this case is an axial **g** tensor whose principal *z* axis makes an angle of about 45° with the direction from copper to the σ-bound axial ligand. This prediction represents the experimental result for M121H for assignment 1 (cf. Table 2). The **g** tensor is nearly axial, and the *z* axis makes an angle of 41° with the Cu−N(His-121) direction.

C. Comparison of the Binding of the Axial Ligand in Azurin, M121H, and M121Q. Here, we discuss the results for M121H in relation to data previously obtained for wild-type azurin and the M121Q mutant of azurin, in which the axial methionine has been replaced by a glutamine. Notwithstanding the similarity of the copper sites of wild-type azurin and its mutants, significant structural differences exist. For azurin, the distance of copper to the equatorial plane spanned by S(Cys-112), N(His-46), and N(His-117) amounts to 0.08 Å[1] and the structure of the copper site of azurin is closest to trigonal. Furthermore, the distance of copper to the axial S(Met-121) is 3.15 Å, indicating that methionine 121 is a weak ligand to copper. When methionine is replaced by a stronger ligand, the copper is pulled out of the equatorial plane (0.56 Å for M121H[11] and 0.26 Å for M121Q[9]) toward the new axial ligand. This is accompanied by a decrease in bond length between copper and the axial ligand (2.24 Å for M121H and 2.25 Å for M121Q).

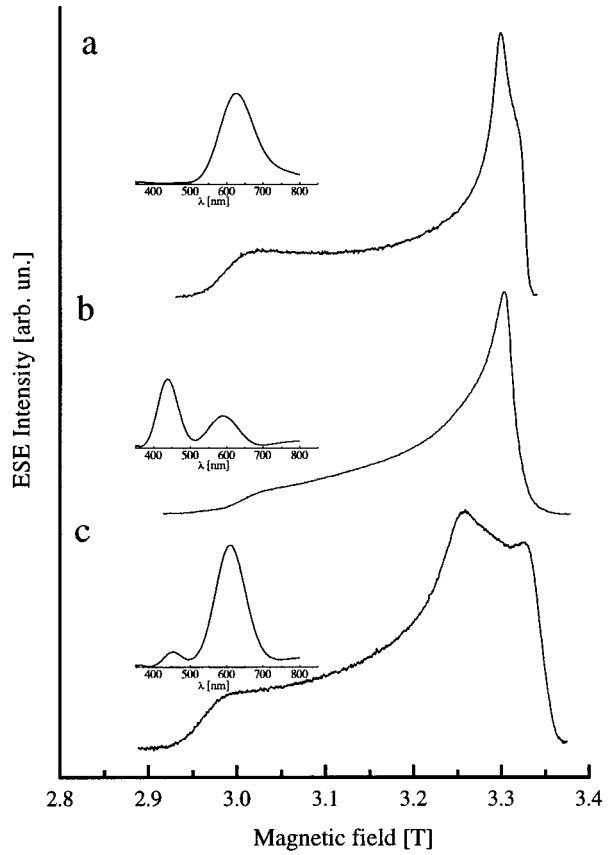

Figure 3. W-band ESE-detected EPR spectra of frozen solutions of azurin (a), M121H (b), and M121Q (c) at 1.2 K. The visible absorption spectra of the respective proteins are included as insets.

The structural differences are linked to subtle differences in the electronic structure, which we will describe in relation to, first, the EPR data and, second, the bands in the visible absorption spectra.

In Figure 3 are represented the ESE-detected EPR spectra at 95 GHz of frozen solutions of azurin and both mutants. The EPR spectrum of azurin is nearly axial, albeit a little less than that of M121H, while the spectrum of M121Q is rhombic. As shown in the previous section, the orientation of the axes system of the **g** tensor in the copper site for M121H is described by assignment 1 in Table 2. The corresponding orientations for azurin and M121Q have been determined previously and summarized in Table 3. We have added in this table the orientation of the *z* axis for *Populus nigra* plastocyanin, the only other data available as yet for a blue-copper protein.[24] Comparison of the proteins reveals a most striking similarity as regards the orientation of the *z* axis. In all cases the direction of the *z* axis is about perpendicular to the plane through copper and the two coordinated nitrogens of the equatorial histidines. While this orientation is conserved, the angle between the *z* axis and the bond between copper and the axial ligand varies from virtually zero to about 45°.

Consideration of the extent of rhombicity of the **g** tensor and the orientation of the principal axes in view of the model presented in the previous section provides insight into the variation of the wave function of the unpaired electron on copper. For azurin, the axial methionine ligand is weakly bound to copper and the nearly axial **g** tensor is derived from the d_{xy} nature of the wave function on copper. In terms of the model this means $A = 1$, and a value of k of 0.036 is needed to reproduce the g_{zz} value of azurin of 2.273. The axial contribution of the orbital on copper to the **g** tensor is compatible with the result of self-consistent-field Xα scattered-wave calculations on a model of the copper site of plastocyanin.[7] According to these calculations, the small rhombicity (0.017) of the **g** tensor of plastocyanin, equal in size to that of azurin, is derived from the part of the wave function that is localized on the sulfur of the cysteine. The *z* principal axis of azurin is found to be perpendicular to the Cu−N(His-46)−N(His-117) plane, which means that the plane of maximum probability amplitude of the d_{xy} orbital is parallel to this plane. Because the sulfur of cysteine-112 is about in this plane as well, the *xy* plane will, to good approximation, coincide with the NNS plane, thereby optimizing the σ overlap of the d_{xy} orbital with the lone pair orbitals of the nitrogens and the π overlap of the d_{xy} orbital with the 3p orbital of sulfur. The resulting picture of the wave function of the unpaired electron is schematically represented in parts a and b of Figure 4 and conforms to that obtained for plastocyanin by various quantum chemical methods.[13,14,25]

For M121H, the model presented in the previous section indicated that the wave function of the unpaired electron on copper comprises the d_{xy} orbital with a small admixture of the d_{yz} orbital, $A \gg B$, $C = D = E = 0$ (strictly speaking, a linear combination of the d_{yz} and the d_{xz} orbital, but in our axes system the nitrogen of histidine 121 is almost in the *yz* plane). The *z* principal axis is, to a good approximation, perpendicular to the Cu−N(His-46)−N(His-117) plane (cf. Figure 4c), and the angle of 41° with the Cu−N(His-121) direction indicates the σ character of the Cu−N(His-121) bond.

For M121Q, the rhombicity of the **g** tensor, the orthogonality of the *z* axis to the Cu−N(His-46)−N(His-117) plane, and the small angle of 10° between the direction of the *z* axis and the Cu−O(Gln-121) (cf. Figure 4d) direction indicate an admixture of d_{z^2} character into the wave function of the unpaired electron. These observations nicely follow the predictions of our model with $A \gg E$ ($B = C = D = 0$). The *z* axis is perpendicular to the *xy* plane and the rhombicity is derived from the *xy* and *yx* elements of the $\mathbf{g}^2$ matrix (cf. eq 5). The admixture of d_{z^2} character has been proposed previously for stellacyanin based on quantum chemical calculations[16,26] on the copper site of this blue-copper protein with an EPR spectrum similar to that of M121Q.

In the insets of Figure 3, the electronic absorption spectra are shown for azurin, M121H, and M121Q. The absorption spectrum of azurin is characterized by an intense absorption at 625 nm, which gives rise to the blue color of the protein. The absorption spectrum of M121H contains two absorptions at 440 and 590 nm, which give the protein its green color. Finally, the absorption spectrum of M121Q shows an intense band at 610 nm and a minor band at 450 nm. For blue-copper proteins, the absorption band at about 600 nm has been ascribed to a ligand-to-metal charge-transfer transition in which one electron is promoted from the doubly occupied orbital that is $Cu(d_{xy})-S(p_{\pi})$ bonding to the orbital of the unpaired electron.[12] Similarly, the band at 450 nm is ascribed to a ligand-to-metal charge-transfer transition[16] in which an electron is promoted from the doubly occupied orbital that is $Cu(d_{x^2-y^2})-S(p_{\sigma})$ bonding to the orbital of the unpaired electron. The intensity of the absorption

(23) Gerloch, M.; Meeking, R. F. *J. Chem. Soc., Dalton Trans.* **1975**, 2443−2451.
(24) Penfield, K. W.; Gay, R. R.; Himmelwright, R. S.; Eickman, N. C.; Norris, V. A.; Freeman, H. C.; Solomon, E. I. *J. Am. Chem. Soc.* **1981**, *103*, 4382−4388.
(25) Shadle, S. E.; Penner-Hahn, J. E.; Schugar, H. J.; Hedman, B.; Hodgson, K. O.; Solomon, E. I. *J. Am. Chem. Soc.* **1993**, *115*, 767−776.
(26) LaCroix, L. B.; Randall, D. W.; Nersissian, A. M.; Hoitink, C. W. G.; Canters, G. W.; Valentine, J. S.; Solomon, E. I. *Biochemistry* **1998**, *35*, 2429−2436.

Table 3. Angles (deg) between the Bond Direction of Copper and Its Ligating Atoms in the Copper Sites of Wild-Type Azurin,[6] M121Q,[20] and Plastocyanin[24] and the Principal Axes of the **g** Tensor (*xyz*)

azurin				M121Q				plastocyanin	
	x	*y*	*z*		*x*	*y*	*z*		*z*
Cu−N(His46)	19	109	90	Cu−N(His46)	8	83	93	Cu−N(His37)	91
Cu−S(Cys112)	113	24	97	Cu−S(Cys112)	145	61	108	Cu−S(Cys84)	104
Cu−N(His117)	125	145	89	Cu−N(His117)	94	175	87	Cu−N(His87)	102
Cu−S(Met121)	79	99	15	Cu−O(Gln121)	87	80	10	Cu−S(Met92)	5

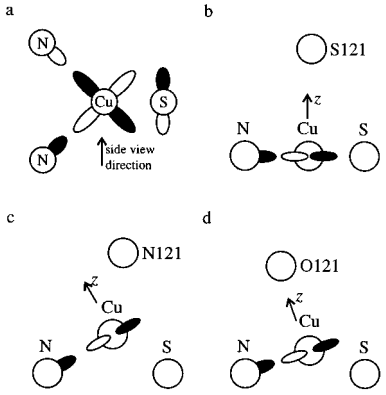

Figure 4. Schematic representation of the coordination of copper in azurin (a, b), M121H (c), and M121Q (d). In (a), a top view of the equatorial NNS plane is given for azurin, while (b), (c), and (d) are side views. Included are the d_{xy} orbital on copper, the lone pair orbitals on the nitrogens, the 3p orbital on sulfur, and the direction of the *z* principal axis of the **g** tensor.

at 450 nm is indicative of the amount of Cu($d_{x^2-y^2}$)−S(p_σ) antibonding character of the singly occupied orbital in the ground state.

The conclusions drawn from the analysis of the EPR spectra concerning the wave function of the unpaired electron corroborate recent suggestions as regards the origin of the 450 nm band. The orthogonality of the *z* axis of the **g** tensor to the Cu−N(His-46)−N(His-117) plane for all three proteins reveals that the σ bonds between the d_{xy} orbital and the lone pair orbitals on the nitrogens of histidines 46 and 117 are conserved. For M121H, as opposed to azurin, the sulfur of the cysteine is not in this plane. The wave function of the unpaired electron has less Cu(d_{xy})−S(p_π) character and acquires Cu($d_{x^2-y^2}$)−S(p_σ) character that shows up in the absorption spectrum of M121H where the band at 450 nm is dominant. This is in line with the more tetrahedral environment for M121H, for which four σ bonds to the ligands are expected. The admixture of a $d_{x^2-y^2}$ component is also compatible with the interpretation of the **g** tensor. According to our model, the *xz* and *yz* elements of the $\mathbf{g}^2$ matrix have a term that contains the coefficient D (for $E = 0$), in combination with B or C. Because both B and C are small, even a sizable admixture of $d_{x^2-y^2}$ does not influence the **g** tensor significantly, provided $D \ll A$. For M121Q, the minor band at 450 nm indicates that the wave function also acquires Cu($d_{x^2-y^2}$)−S(p_σ) character, albeit to a lesser extent.

Conclusion

The electronic structure of the copper site of the M121H mutant of azurin, for which the axial methionine 121 is replaced by a histidine, has been investigated by pulsed EPR at 95 GHz on a single crystal. The complete **g** tensor has been determined. It is nearly axial, and the direction of the *z* principal axis is perpendicular to the plane through copper and the coordinated nitrogens of histidines 46 and 117 and makes an angle of 41° with the direction of copper to N(His-121).

The wave function of the unpaired electron on copper primarily comprises a d orbital (d_{xy} in our axes system) that makes σ interactions with the lone pair orbitals on the nitrogens and a π interaction with a 3p orbital on the sulfur. Analysis of the **g** tensor for M121H shows that d_{yz} character mixes into this wave function. This admixture does not introduce rhombicity into the **g** tensor, and the copper is σ-bound to the nitrogen of the axial histidine 121 through the d_{yz} orbital. This is in contrast with the M121Q mutant of azurin and stellacyanin for which the axial glutamine is σ-bound through the d_{z^2} orbital. The admixture of the d_{z^2} orbital introduces rhombicity into the **g** tensor.

The observation for azurin and the mutants M121H and M121Q that the *z* axis is perpendicular to the plane spanned by copper and the nitrogens of the strongly coupled histidines 46 and 117 reveals that the σ bonds of the d_{xy} orbital to the nitrogens are conserved while the π bond to the sulfur of cysteine 112 weakens when the copper gets further from the N(His-46)−N(His-117)−S(Cys-112) plane.

Analysis of the rhombicity (or the lack thereof) allows for the characterization of the d orbital that is involved in the binding of the axial ligand. The admixture of d_{yz} (M121H) or d_{z^2} (M121Q) character into the wave function is small but induces substantial changes in the EPR and electronic absorption spectra. The subtle differences in the electronic structure are not one-to-one related to the identity of the axial ligand or to the distance of copper to the NNS plane. For example, the blue-copper protein pseudoazurin, which has methionine as its axial ligand, is characterized by an EPR spectrum similar to those of stellacyanin and M121Q. For the blue-copper protein plastocyanin, the distance of copper to the NNS plane (0.34 Å) is larger than that for M121Q (0.26 Å). Yet, the EPR and electronic absorption spectra are very similar to those of azurin for which this distance is small (0.08 Å). Quantum chemical studies are necessary to allow generalizations about the electronic structure of blue-copper proteins. Such investigations are in progress in our laboratory, and the **g** tensor and hyperfine[18,19,27] data from EPR studies enable a critical judgment of the calculated wave function.

Acknowledgment. The authors thank J. Mol and J. W. A. Coremans for their help during the initial stage of this project. This work has been performed under the auspices of the Biomac Research School of the Leiden and Delft Universities and was supported with financial aid by The Netherlands Organization for Scientific Research (NWO), department Chemical Sciences (CW).

JA993357F

(27) van Gastel, M.; Coremans, J. W. A.; Mol, J.; Jeuken, L. J. C.; Canters, G. W.; Groenen, E. J. J. *JBIC, J. Biol. Inorg. Chem.* **1999**, *4*, 257−265.